Theoretical Study on Cystine-Based Cyclobisamides

Francesco Ferrante and Gianfranco La Manna*

Dipartimento di Chimica Fisica, Università degli Studi, Viale delle Scienze, 90128 Palermo, Italy

Received: March 27, 2002; In Final Form: June 12, 2002

Nanotubular structures made of cystine-based cyclobisamides assembled by stacking through hydrogen bonding between amidic groups were recently synthesized. A quantum mechanical study at Hartree−Fock and DFT levels was performed on such monomers and dimers, and the obtained geometrical data were compared with the corresponding experimental values on the polymers. The electrostatic potential derived from the wave function seems to be a suitable tool for testing the ability to form hydrogen bonds and, as a consequence, for suggesting the synthesis of new nanotubes with different structural units providing efficient hydrogen-bonding stacking interactions.

1. Introduction

The increasing interest in designing open-ended hollow tubular structures of molecular dimensions, constructed from organic molecules, is caused by their unique functional properties, ranging from catalysis to the use as selective transporting systems.[1−6]

We have focused our attention on tubular structures set up by the association of cyclic peptide units,[7−11] which show their utility as solubilizers, vectors for controlled drugs releasing, and selective sensors.[12−15]

The existence of these systems was inferred many years ago;[16−18] nowadays, several cyclopeptide-based tubular structures are known, which are self-assembled through a stacking process that is affected by the size and the shape of the peptide subunit.[19−22] Recently, it was found that similar tubular systems can be built through the self-assembly of cyclic systems obtained from the condensation of cystine with a bicarboxylic acid. These cystine-based cyclobisamides,[23,24] having the amide groups at the opposite side of the ring, are very efficient units for obtaining tubular structures by the formation of intermolecular antiparallel hydrogen bonds between the CO and NH groups of two adjacent units.

Theoretical ab initio calculations concerning the structural features of such compounds are almost absent in the literature, except for two papers on the monomers and dimers of cyclo-[(Gly-D-Ala)$_4$][20] and cyclo[(L-Phe-D-Ala)$_n$],[22] respectively.

In this article, ab initio calculations are reported on the equilibrium structure and electronic properties of the cystine-based cyclobisamides, CBA*n* (−CO−(CH$_2$)$_n$−CO−cyst−) where cyst = (−NH−CH(CO$_2$Me)−CH$_2$−S−)$_2$, which is the single unit of the open-ended tubular structures here considered for *n* = 4, 5, and 6. A comparison is made between the experimental data obtained in the solid phase and the geometrical structure derived from ab initio calculations, because a substantial agreement between theoretical and experimental results is essential for further theoretical studies on the aggregates. Starting from the optimized geometry of the monomer, we also performed calculations on CBA4 dimers.

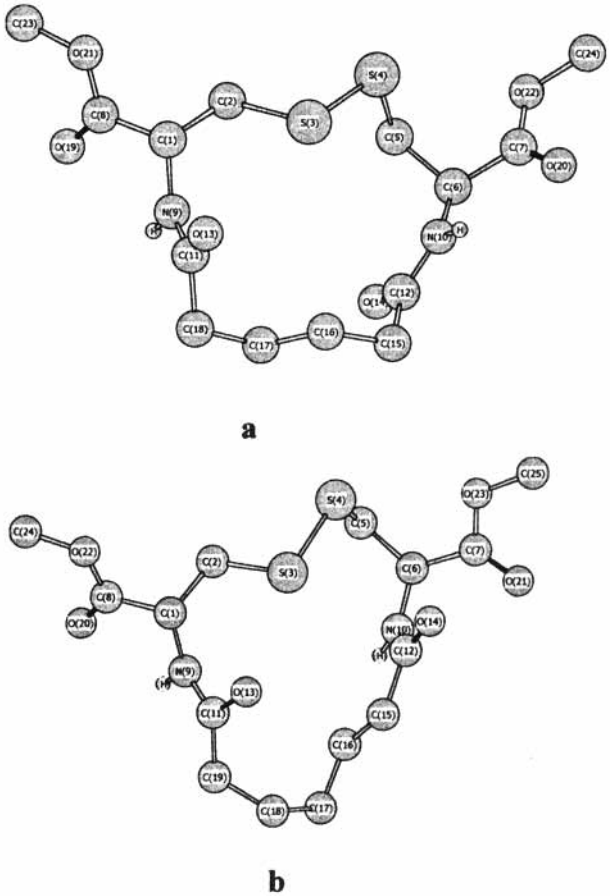

Figure 1. Optimized structures and atom-numbering scheme of (a) CBA4 and (b) CBA5. For the sake of clarity, only hydrogen atoms bound to nitrogen are shown.

2. Method of Calculation

All calculations on the monomers were performed at Hartree−Fock (HF) level with the split-valence 6-31G** basis set by using the program package Gaussian 98W[25]. The geometries of the considered systems were fully optimized as concerns the monomers by checking the Hessian matrix eigenvalues; optimizations beyond the HF level were not performed because of the size of the studied systems. DFT calculations were also

* To whom correspondence should be addressed. E-mail address: lamanna@unipa.it. Fax number: +39-91590015.

10.1021/jp020821l CCC: $25.00
Published on Web 12/05/2002

TABLE 1: Optimized Geometric Parameters (in Å and deg) of CBA4 and CBA5

	$n = 4$			$n = 5$
	HF	DFT	expt[a]	HF[b]
C1−C2	1.541	1.548	1.546	1.541
C2−S3	1.826	1.853	1.818	1.823
S3−S4	2.053	2.084	2.025	2.051
S4−C5	1.826	1.846		1.822
C5−C6	1.535	1.543		1.537
C1−N9	1.437	1.445		1.443
C6−N10	1.441	1.447		1.442
C1−N9	1.437	1.445		1.443
N9−C11	1.358	1.370		1.358
N10−C12	1.353	1.365		1.358
C11−O13	1.202	1.228		1.201
C12−O14	1.206	1.231		1.200
C11−C18	1.516	1.522		1.520 (C11−C19)
C12−C15	1.517	1.523		1.521
C17−C18	1.539	1.546		1.538 (C19−C18)
C15−C16	1.539	1.545		1.531
C16−C17	1.531	1.535		1.535 (C18−C17)
C1−C8	1.521	1.529		1.521
C6−C7	1.521	1.526		1.529
C8−O19	1.189	1.213		1.190 (C8−O20)
C7−O20	1.188	1.213		1.186 (C7−O21)
C8−O21	1.317	1.342		1.315 (C8−O22)
C7−O22	1.318	1.342		1.316 (C7−O23)
N9···N10	5.317	5.433	5.50	5.005
S3···C16	4.192	4.200	3.95	5.447 (S3···C17)
C1−C2−S3	110.6	111.1	111	110.1
C2−S3−S4	101.7	101.0	101	102.8
S3−S4−C5	105.4	105.3	105	106.1
S4−C5−C6	116.1	115.9	114	121.5
C1−C2−S3−S4	172.4	171.9	176	180.
C2−S3−S4−C5	−88.7	−89.2	−90	−84.5
S3−S4−C5−C6	−87.1	−88.3	−93	−73.7
S4−C5−C6−N10	72.4	71.9		68.8
C5−C6−N10−C12	77.1	74.8		−88.8
C7−C6−N10−C12	−156.8	−159.1		46.7
N10−C6−C7−O22	−179.3	−178.5	−166	−137.9 (N10−C6−C7−O23)
N9−C1−C8−O21	162.8	166.9	179	165.4 (N9−C1−C8−O22)
N10−C12−C15−C16	94.3	98.0	86	−9.6
N9−C11−C18−C17	76.0	83.5	82	144.1 (N9−C11−C19−C18)
O13−C11−N9−H31	−170.9	−169.6		−169.3
O14−C12−N10−H32	−173.5	−172.7		177.9

[a] X-ray diffraction data on poly-CBA4.[23] [b] The correct numbering is reported in parentheses for CBA5, where necessary.

carried out with the same basis set using the B3LYP parametrization.[26] Vibrational frequency values in the harmonic approximation were calculated at HF and DFT levels and scaled according to the prescriptions found in the literature.[27,28] In the case of CBA4 dimer, single-point ab initio calculations were carried out, as well as a full geometry optimization at HF level.

3. Results and Discussion

A. Monomers. The adopted numbering scheme of the cystine-based cyclobisamides, CBA*n* (−CO−$(CH_2)_n$−CO−cyst−) where cyst = (−NH−CH(CO_2Me)−CH_2−S−)$_2$ and n = 4 or 5, is reported in Figure 1. The compound with $n = 4$ is the smallest monomeric unit among the cystine-based cyclobisamides studied by Ranganathan et al.,[23,24] who synthesized polymeric structures derived from the assembling of monomers having an even number of CH_2 groups (n = 4, 6, 8, 10, and 20) and obtained structural data by X-ray diffraction on the solid phase.

The relevant geometrical parameters obtained from the optimization for the monomers with $n = 4$ and 5 along with the available experimental data, which concern only the polymeric structure with $n = 4$, are reported in Table 1.

When n is an odd number, the products were not obtained in crystal form preventing a comparison with experimental data in the case $n = 5$. The agreement between the theoretical results and the experimental data at HF and DFT levels is satisfactory, considering that the computed data were obtained for the monomer, whereas the experimental results concern polymeric structures in the solid phase. This indicates that the geometrical parameters concerning the structure of the CBA4 monomer are slightly changed when the polymeric structure is formed. The maximum deviation between theoretical and experimental values is 0.06 Å for bond lengths, 4° for bond angles, and 16° for torsional angles. The size of the cavity area inside the structure is also well evaluated, given that the N9···N10 distance is underestimated by about 1−3% whereas the S3···C16 distance is overestimated by about 5−6%. It is to be observed that CBA4 is not a symmetric structure because of the valency state of the sulfur atoms.

When the considered system is CBA6, the larger size of the cycle allows for a conformational flexibility, giving rise to some local minima corresponding to different conformers. The geometrical data obtained from theoretical calculations are reported in Table 2, along with the experimental values in the solid phase on the polymeric structure; the resulting structures of the systems are shown in Figure 2. It is quite evident, both from the numerical values of the geometrical parameters and from the observation of the depicted structures, that the

TABLE 2: Optimized Geometric Parameters (in Å and deg) of the Conformers of CBA6 at HF/6-31G Level**

	I	II	III	expt[a]
HF energy (au)	−1974.2375	−1974.2394	−1974.2502	
ΔE (kJ mol^{-1})	+33.4	+28.4	0.0	
C1−C2	1.534	1.538	1.534	1.522
C2−S3	1.829	1.819	1.819	1.819
S3−S4	2.056	2.060	2.057	2.017
S4−C5	1.829	1.822	1.822	1.819
C5−C6	1.531	1.532	1.532	1.525
C1−N9	1.435	1.440	1.437	
C6−N10	1.438	1.451	1.446	
N9−C11	1.359	1.357	1.364	
N10−C12	1.366	1.363	1.359	
C11−O13	1.200	1.205	1.202	
C12−O14	1.200	1.199	1.201	
C11−C20	1.517	1.519	1.517	
C12−C15	1.517	1.515	1.518	
C19−C20	1.541	1.535	1.531	
C15−C16	1.539	1.540	1.534	
C16−C17	1.532	1.534	1.535	
C17−C18	1.540	1.537	1.534	
C19−C20	1.541	1.535	1.531	
C1−C8	1.527	1.525	1.527	
C6−C7	1.527	1.527	1.523	
C8−O21	1.186	1.189	1.188	
C7−O22	1.189	1.190	1.191	
C8−O23	1.318	1.316	1.318	
C7−O24	1.315	1.315	1.313	
N9···N10	4.795	5.295	5.104	
C5···C18	6.644	5.923	5.214	
C1−C2−S3	110.9	116.5	116.6	115
C2−S3−S4	105.3	103.3	103.6	104
S3−S4−C5	102.5	102.9	103.2	103
S4−C5−C6	117.0	114.1	114.1	112
C1−C2−S3−S4	163.6	−78.0	−67.4	−53
C2−S3−S4−C5	−80.9	97.9	99.1	97
S3−S4−C5−C6	−83.8	84.2	72.6	101
S4−C5−C6−N10	70.7	−153.3	−171.5	
C5−C6−N10−C12	139.3	127.4	125.2	
C7−C6−N10−C12	−93.0	−109.7	−114.2	−136
N9−C1−C8−O23	−31.5	161.9	165.8	157
N10−C12−C15−C16	75.5	114.8	147.7	125
N9−C11−C20−C19	−54.6	−154.2	173.4	141
C8−C1−N9−C11	−66.1	−114.1	−89.6	−75

[a] X-ray diffraction data on poly-CBA6.[23]

conformer III is the most similar to the structure found in the solid, especially in the region of the amidic groups, which are the centers responsible for the hydrogen bonds allowing the stacking process. In particular, the examination of the dihedral angle values enables us to rule out that the experimental structure can be described from the conformers I and II.

For obtaining some supplementary information on the ability of the monomers to form hydrogen bonds, the molecular electrostatic potential (MESP), obtained from the HF wave functions, can be utilized. The electrostatic isopotential contour maps for the conformers II and III in a plane crossing the carbon atoms of the peptide groups are shown in Figure 3. These maps show that an antiparallel hydrogen bonding between the peptide groups of different monomers along the axis of the nanotube is correctly aligned only in the case of the conformer III. In fact, the shape of the contour lines obtained in the case of the conformer II does not seem to allow for an efficient hydrogen-bonding interaction.

The calculated harmonic vibrational frequencies for CBA4 are reported in Table 3. No experimental IR data were found in the literature for a comparison with the theoretical values. A qualitative assignment of the vibrational normal modes is also reported.

The DFT frequency values corresponding to the NH stretching mode are slightly larger than those reported in the literature for

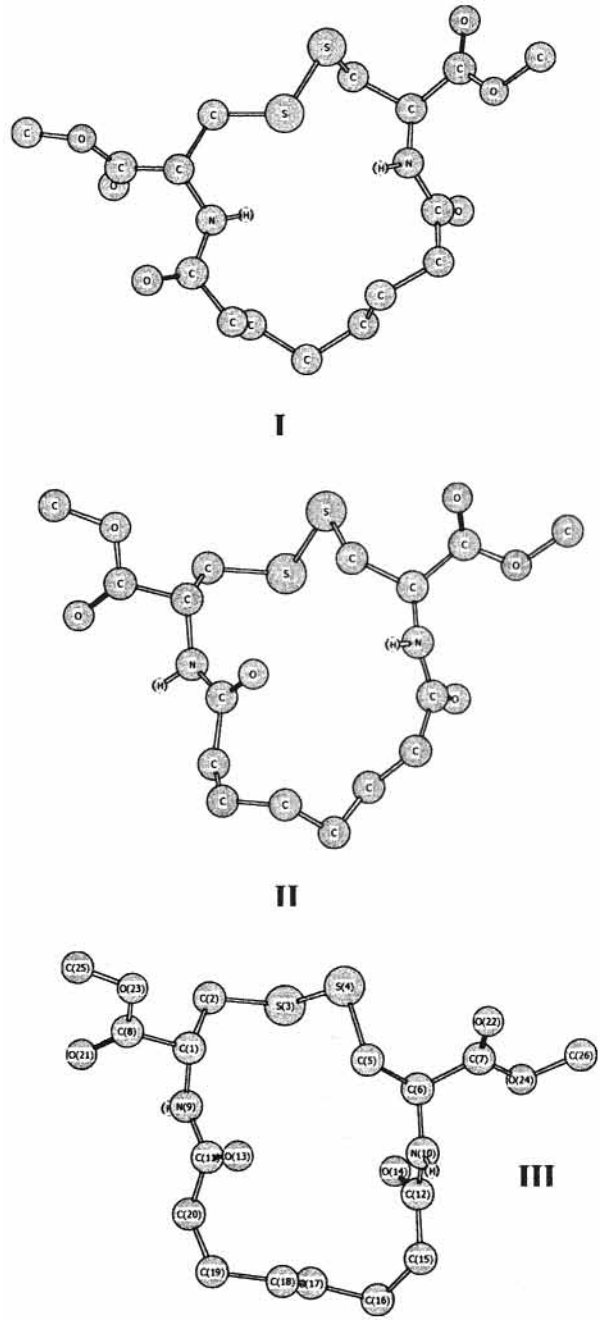

Figure 2. Optimized structures and atom numbering scheme of the three conformers of CBA6. For sake of clarity, only hydrogen atoms bound to nitrogen are shown.

monomeric cyclopeptides,[20,22] whereas the opposite occurs for the amidic CO stretching mode. The frequency values obtained at DFT level are predicted larger than HF values in the case of N−H and C−H stretching modes and lower in the other cases; the differences are generally about 2−3% and all below 100 cm^{-1}.

B. Dimers. An attempt to simulate the structure of the polymeric CBA4 was performed by bringing together two CBA4 units along the *z* axis, perpendicular to the average planes of the monomers. Single-point HF calculations were carried out for some values of the distance between the average planes of the two monomers (h), the relative rotation angle about the *z* longitudinal axis (φ), and the displacements along the two perpendicular *x* and *y* axes, d_x and d_y, respectively. The corresponding interaction energy values were obtained after correction of the BSSE by the counterpoise method[29] and are

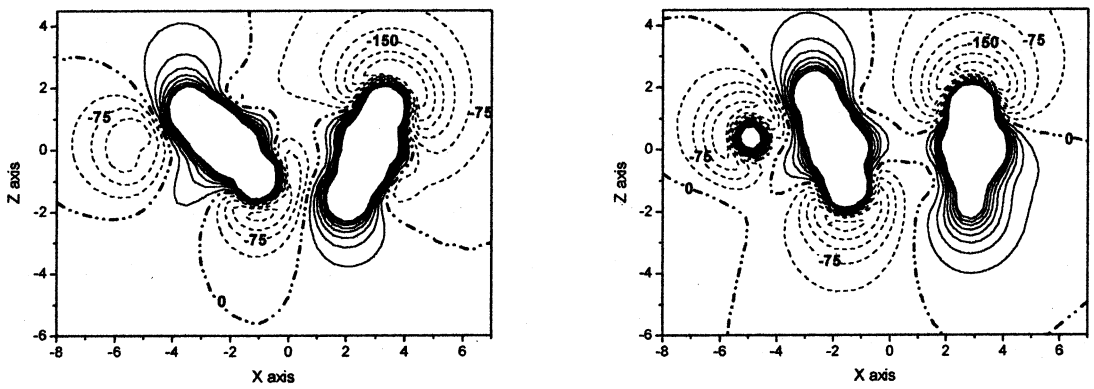

Figure 3. Electrostatic isopotential contour maps of the conformers II (left) and III (right) of CBA6 for a section crossing the peptidic CO groups. Values are given in kcal mol^{-1}. Solid lines correspond to positive values and dashed lines to negative values. The difference between two successive contours is about 33 kcal mol^{-1}.

TABLE 3: Calculated Vibrational Frequencies (cm^{-1}) for CBA4

HF[a]	DFT[b]	qualitative assignment
3476, 3472	3483, 3477	N−H stretching
2978(2), 2963, 2960, 2885, 2883	3061, 3060, 3031, 3029, 2953, 2952	C−H stretching (ester methyl groups)
2970, 2951, 2940, 2927, 2918, 2910, 2907, 2900, 2884, 2871, 2867, 2863, 2853, 2852	3040, 3023, 2998, 2990(2), 2974, 2971(2), 2954, 2935, 2934, 2925, 2923, 2903	C−H stretching (methylene groups)
1795, 1792	1752, 1749	C−O stretching (ester groups)
1741, 1721	1693, 1682	C−O stretching (amidic groups)
1523, 1516	1480, 1450	H−N−C bending
1458, 1451, 1449, 1446, 1392	1444, 1439, 1438, 1425, 1328	H−C−H bending (methylene groups)
1457(2), 1450(2), 1448, 1447	1441, 1439, 1427, 1426, 1399	H−C−H bending (ester groups)
523	471	S−S stretching

[a] Frequency values scaled by 0.8929. Degeneracy given in parentheses. [b] Frequency values scaled by 0.9613. Degeneracy given in parentheses.

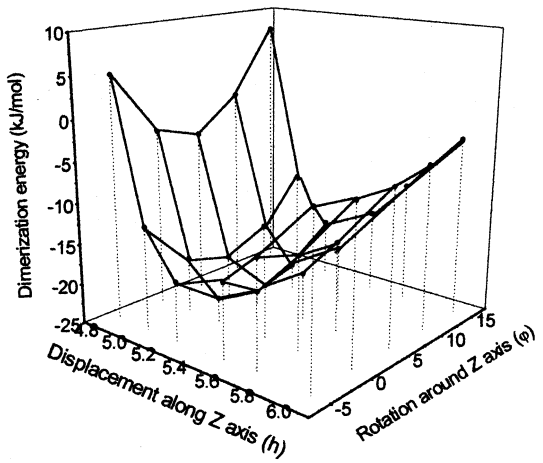

Figure 4. Interaction energy values (kJ mol^{-1}) of the CBA4 dimer as a function of the distance between the monomers (h, Å) and the rotation angle around the longitudinal axis (φ, deg).

depicted in Figure 4, in which only the variables h and φ are considered, given that the starting values $d_x = d_y = 0$ correspond to the minimum energy value.

TABLE 4: Relevant Geometric Parameters (in Å and deg) Involving the Intermolecular Hydrogen Bonding of (CBA4)$_2$[a]

	partial optim[b]	expt	full optim
$O_a\cdots H_b$	2.344	2.06	2.184
$O_a\cdots H_b-N_b$	163.0		164.6
$C_a-O_a\cdots H_b$	165.0		164.4
$C_a-O_a\cdots H_b-N_b$	−151.6		174.9
$H_a\cdots O_b$	2.573	2.13	2.307
$N_a-H_a\cdots O_b$	147.1		156.7
$H_a\cdots O_b-C_b$	146.3		158.8
$N_a-H_a\cdots O_b-C_b$	−175.4		−176.6
$N_a\cdots O_b$	3.449	3.002	3.248
$N_b\cdots O_a$	3.307	2.948	3.159
$N_a\cdots O_b-C_b$	155.3	166.0	165.8
$N_b\cdots O_a-C_a$	169.2	167.2	169.2

[a] The subscripts a and b refer to the two monomeric units. [b] Optimization only for intermolecular geometrical parameters.

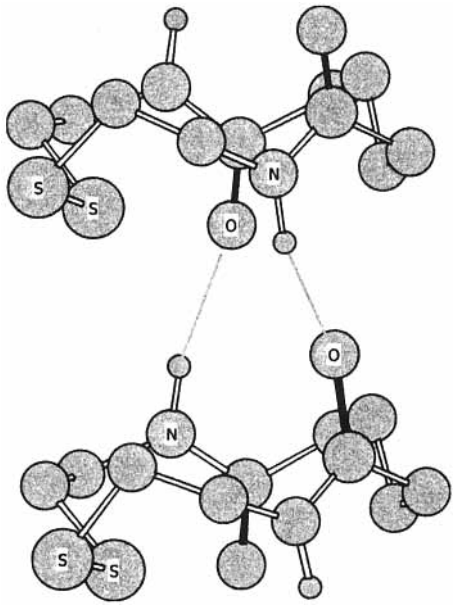

Figure 5. Optimized structure of the CBA4 dimer. Outer ester groups are not shown; only hydrogen atoms bound to nitrogen are depicted.

The maximum value of the dimerization energy, corresponding to 23 ± 1 kJ mol^{-1} (about 11 kJ mol^{-1} per H bond), was found at $h = 5.2 \pm 0.1$ Å and $\varphi = 5° \pm 2°$. The relevant intermolecular geometrical parameters involving the hydrogen bonds that are responsible for the stacking interaction are reported in Table 4, along with the available experimental data. The calculated values of the hydrogen bond distances, larger by about 15% than the experimental ones, seem to indicate the

TABLE 5: Optimized Geometric Parameters (in Å and deg) of the CBA4 Dimer at HF/6-31G Level[a]**

	monomer a	monomer b
C1−C2	1.541	1.542 (+0.001)
C2−S3	1.826	1.827 (+0.001)
S3−S4	2.053	2.053
S4−C5	1.825 (−0.001)	1.825
C5−C6	1.538 (+0.003)	1.535
C1−N9	1.439 (+0.002)	1.435 (−0.002)
C6−N10	1.437 (−0.004)	1.441
N9−C11	1.350 (−0.008)	1.357 (−0.001)
N10−C12	1.353	1.345 (−0.008)
C11−O13	1.207 (+0.005)	1.204 (+0.002)
C12−O14	1.208 (+0.002)	1.211 (+0.005)
C11−C18	1.515 (−0.001)	1.515 (−0.001)
C12−C15	1.515 (−0.002)	1.517
C17−C18	1.541 (+0.002)	1.538 (−0.001)
C15−C16	1.537 (−0.002)	1.541 (+0.002)
C16−C17	1.531	1.530 (−0.001)
C1−C8	1.522 (+0.001)	1.520 (−0.001)
C6−C7	1.517 (−0.004)	1.518 (−0.003)
C8−O19	1.189	1.190 (+0.001)
C7−O20	1.184 (−0.004)	1.189 (+0.001)
C8−O21	1.316 (−0.001)	1.319 (+0.002)
C7−O22	1.319 (+0.001)	1.318
N9···N10	5.364 (+0.047)	5.336 (+0.019)
S3···C16	4.239 (+0.047)	4.176 (−0.016)
C1−C2−S3	110.6	110.5 (−0.1)
C2−S3−S4	101.9 (+0.2)	101.7
S3−S4−C5	105.3 (−0.1)	105.5 (+0.1)
S4−C5−C6	116.2 (+0.1)	116.3 (+0.2)
C1−C2−S3−S4	172.4	173.5 (+1.1)
C2−S3−S4−C5	−92.7 (−4.0)	−88.6 (+0.1)
S3−S4−C5−C6	−86.3 (+0.8)	−86.5 (+0.6)
S4−C5−C6−N10	74.4 (+2.0)	73.7 (+1.3)
C5−C6−N10−C12	78.6 (+1.5)	81.0 (+3.9)
C7−C6−N10−C12	−154.3 (+2.5)	−153.2 (+3.6)
N10−C6−C7−O22	178.7 (−2.0)	−179.0 (+0.3)
N9−C1−C8−O21	168.3 (+5.5)	157.8 (−5.0)
N10−C12−C15−C16	88.9 (−5.4)	87.4 (−6.9)
N9−C11−C18−C17	80.9 (+4.9)	77.2 (+1.2)
O13−C11−N9−H31	−172.2 (−1.3)	−174.9 (−4.0)
O14−C12−N10−H32	−178.6 (−5.1)	−175.6 (−2.1)

[a] Differences with respect to the corresponding values found in the monomer (see Table 1) are reported in parentheses.

necessity of a full geometry optimization on the dimer. In other words, the arrangement corresponding to an optimal stacking interaction between the two CBA4 monomers should require some geometrical changes within the structure of the monomers.

The computation, on a system made up of 92 atoms, took more than 300 h on a Pentium IV, 1.8 GHz processor, giving rise to an optimized structure, shown in Figure 5, the details of which are reported in Table 5. The energy gain, with respect to the isolated monomers, obtained from the full optimization of the dimer increased by about 30 kJ mol^{-1}. The comparison of the intermolecular parameters with the experimental values (Table 4) allows us to point out that the H-bond distances are noticeably decreased, and closer to the experimental values, as a consequence of small geometrical variations within the monomers, which essentially concern the dihedral angle values referring to the peptidic groups and to outer ester groups. These geometrical rearrangements are consistent with more efficient antisymmetrical H-bonds, as outlined from the values of the C−O···H−N dihedral angles in the fully optimized structure ($C_a-O_a\cdots H_b-N_b$ close to the $N_a-H_a\cdots C_b-O_b$ with the opposite sign). It is worthwhile to outline that, in the polymeric structure, both NH and CO groups of each monomeric moiety are involved in the H-bond formation, one with the adjacent upper moiety and another with the lower moiety, whereas the truncation of the system to a dimeric structure allows just two hydrogen bonds

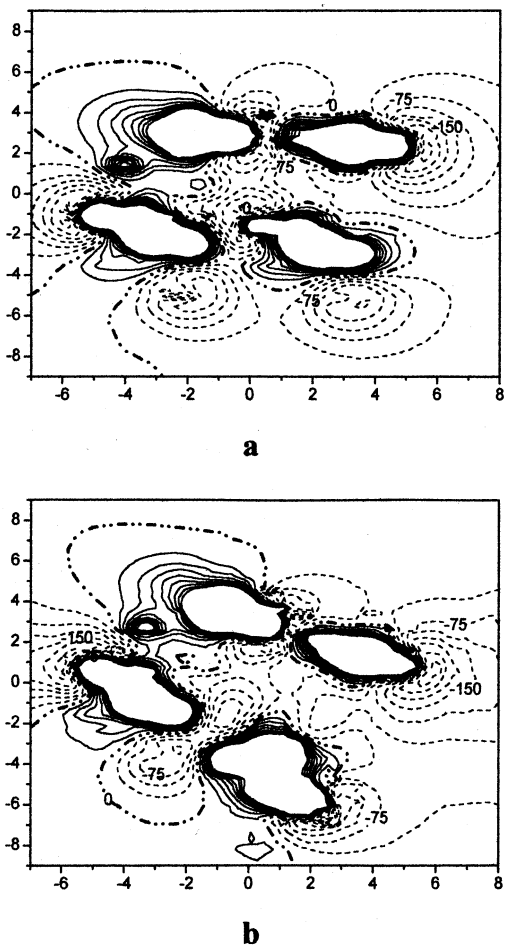

Figure 6. Electrostatic isopotential contour maps of $(CBA4)_2$ after (a) partial optimization and (b) full optimization. Values are given in kcal mol^{-1}. Solid lines correspond to positive values and dashed lines to negative values. The difference between two successive contours is about 33 kcal mol^{-1}.

TABLE 6: Calculated Electrostatic Potential at the Oxygen and at the Hydrogen[31] in Isolated CBA4 and Corresponding Variations When Considering the Monomers Having the Geometry as Found in the Dimer (Values in au)

atom A	V_A (isolated CBA4)	ΔV_A(CBA4a) [a]	ΔV_A (CBA4b)[a]
O13	−22.3549	−0.0025 (H-bond)	+0.0008
O14	−22.3531	−0.0009	−0.0024 (H-bond)
H (bound to N9)	−1.0177	+0.0007	+0.0056 (H-bond)
H (bound to N10)	−1.0173	+0.0011 (H-bond)	−0.0020

[a] a and b are the symbols defining the two monomers in the dimer.

to be formed. So, when the dihedral angle values obtained from the dimer optimization are compared with the experimental values in the polymer (Table 1), the agreement with respect to the optimized values in the monomer is improved, as expected, only in the regions involved in the H-bond formation.

A further evidence is obtainable from the comparison of the electrostatic isopotential maps derived from the wave functions corresponding to the partial and fully optimized $(CBA4)_2$ structures reported in Figure 6. The MESP values in the region between the NH and CO groups (lower part of the Figure 6a,b) are quite different and suggest a substantial difference in the hydrogen-bond energies. In particular, the electrostatic potential at the nuclei[30,31] (EPN) of oxygen and hydrogen, involved in the hydrogen bonds, evaluated at the optimized geometry of the CBA4 monomer as isolated molecule, as well as at the geometry assumed in the dimer, enables us to make some

quantitative considerations. These data, reported in Table 6, show that each time that the oxygen atom is involved in the formation of a hydrogen bond the EPN at the oxygen noticeably decreases when passing from the isolated CBA4 to the monomer in the dimer; in contrast, an increase of EPN occurs in the case of the hydrogen atom. This behavior, corresponding to an enhancement of the hydrogen-bond energy,[30] confirms that slight modifications of the geometry of the monomers can induce a significant improvement in the hydrogen-bond energy.

This result suggests that the research on novel monomeric units suitable for the construction of tubular nanotubes should take into account the information provided from the evaluation of the EPN at the atoms involved in the hydrogen bonds responsible for the stacking interaction.

4. Conclusions

Monomers and dimers of cystine-based cyclobisamides were theoretically studied by ab initio HF and DFT methods. The obtained results show that a full optimization of the dimer is able to reproduce, at least at a qualitative level, the main geometrical features of the nanotubular aggregate, which is obtained from self-association by the stacking process driven from H-bond formation between peptidic units.

The examination of the electrostatic potential seems to be a valuable tool for providing a qualitative evaluation of the efficiency of the H-bonds to be formed between the monomeric units. This should be particularly useful when examining different monomeric units within similar classes of compounds to suggest new, not yet synthesized tubular structures.

Acknowledgment. This work was supported by Ministry of Education under 60%- 1998 funds.

References and Notes

(1) Iijima, S. *Nature* **1991**, *354*, 56.
(2) Ebbesen, T. W.; Ajayan, P. M. *Nature* **1992**, *358*, 220.
(3) Salahub, D.; Rochefort, A.; Avouris, P. *J. Phys. Chem. B* **1999**, *103*, 641.
(4) Martel, R.; Shea, H.; Avouris, P. *J. Phys. Chem. B* **1999**, *103*, 7551.
(5) Nangia, A. *Curr. Opin. Solid State Mater. Sci.* **2001**, *5*, 115.
(6) Bong, D. T.; Clark, T. D.; Granja, J. R.; Ghadiri, M. R. *Angew. Chem., Int. Ed.* **2001**, *40*, 988.
(7) Ghadiri, M. R.; Granja, J. R.; Milligan, R. A.; McRee, D. E.; Khazanovich, N. *Nature* **1993**, *366*, 324.
(8) Ghadiri, M.; Granja, J. R.; Buehler, L. K. *Nature* **1994**, *369*, 301.
(9) Khazanovich, N.; Granja, J. R.; McRee, D. E.; Milligan, R. A.; Ghadiri, M. R. *J. Am. Chem.* Soc. **1994**, *116*, 6011.
(10) Ghadiri, M. R.; Kobayashi, K.; Granja, J. R.; Chadha, R. K.; McRee, D. E. *Angew. Chem., Int. Ed. Engl.* **1995**, *34*, 93.
(11) Kobayashi, K.; Granja, J. R.; Ghadiri, M. R. *Angew. Chem., Int. Ed. Engl.* **1995**, *34*, 95.
(12) Moerner, W. E.; Kador, L. *Phys. Rev. Lett.* **1989**, *62*, 2535.
(13) Harris, K. *Chem. Soc. Rev.* **1997**, *26*, 279.
(14) Motesharei, K.; Ghadiri, M. R. *J. Am. Chem. Soc.* **1997**, *119*, 11306.
(15) Clark, T. D.; Buehler, L. K.; Ghadiri, M. R. *J. Am. Chem. Soc.* **1998**, *120*, 651.
(16) Hassal, C. H. *Proceedings of the Third American Peptide Symposium;* Meinhoffer, J., Ed; Ann Arbor Science Publishing: Ann Arbor, MI, 1972; pp 153−157.
(17) De Santis, P.; Morosetti, S.; Rizzo, R. *Macromolecules* **1974**, *7*, 52.
(18) Karle, I. L.; Handa, B. K.; Hassal, C. H. *Acta Crystallogr.* **1975**, *B31*, 555.
(19) Hartgerink, J. D.; Granja, J. R.; Milligan, R. A.; Ghadiri, M. R. *J. Am. Chem. Soc.* **1996**, *118*, 43.
(20) Jishi, R. A.; Flores, R. M.; Valderrama, M.; Lou, L.; Bragin, J. *J. Phys. Chem. A* **1998**, *102*, 9858.
(21) Rapaport, H.; Kim, H. S.; Kjaer, K.; Howes, P. B.; Cohen, S.; Als-Nielsen, J.; Ghadiri, M. R.; Leiserowitz, L.; Lahav, M. *J. Am. Chem. Soc.* **1999**, *121*, 1186.
(22) Chen, G.; Su, S.; Liu, R. *J. Phys. Chem. B* **2002**, *106*, 1570.
(23) Ranganathan, D.; Haridas, V.; Sivakama Sundari, C.; Balasubramanian, D.; Madhusudanan, K. P.; Roy R.; Karle, I. L. *J. Org. Chem.* **1999**, *64*, 9230.
(24) Ranganathan, D.; Lakshmi, C.; Haridas, V.; Gopikumar, D. *Pure Appl. Chem.* **2000**, *72*, 365.
(25) Frisch, M. J.; Trucks, G. W.; Schlegel, H. B.; Scuseria, G. E.; Robb, M. A.; Cheeseman, J. R.; Zakrzewski, V. G.; Montgomery, J. A., Jr.; Stratmann, R. E.; Burant, J. C.; Dapprich, S.; Millam, J. M.; Daniels, A. D.; Kudin, K. N.; Strain, M. C.; Farkas, O.; Tomasi, J.; Barone, V.; Cossi, M.; Cammi, R.; Mennucci, B.; Pomelli, C.; Adamo, C.; Clifford, S.; Ochterski, J.; Petersson, G. A.; Ayala, P. Y.; Cui, Q.; Morokuma, K.; Malick, D. K.; Rabuck, A. D.; Raghavachari, K.; Foresman, J. B.; Cioslowski, J.; Ortiz, J. V.; Stefanov, B. B.; Liu, G.; Liashenko, A.; Piskorz, P.; Komaromi, I.; Gomperts, R.; Martin, R. L.; Fox, D. J.; Keith, T.; Al-Laham, M. A.; Peng, C. Y.; Nanayakkara, A.; Gonzalez, C.; Challacombe, M.; Gill, P. M. W.; Johnson, B. G.; Chen, W.; Wong, M. W.; Andres, J. L.; Head-Gordon, M.; Replogle, E. S.; Pople, J. A. *Gaussian 98*, revision A.7; Gaussian, Inc.: Pittsburgh, PA, 1998.
(26) Becke, A. D. *J. Chem. Phys.* **1993**, *98*, 5648.
(27) Pople, J. A.; Scott, A. P.; Wong, M. W.; Radom, L. *Isr. J. Chem.* **1993**, *33*, 345.
(28) Foresman, J. B.; Frisch, E. *Exploring Chemistry with Electronic Structure Methods*, 2nd ed.; Gaussian Inc.: Pittsburgh, PA, 1996; p 64.
(29) Boys, S. F.; Bernardi, F. *Mol. Phys.* **1970**, *19*, 553.
(30) Galabov, B.; Bobadova-Parvanova P. *J. Phys. Chem. A* **1999**, *103*, 6793.
(31) The electrostatic potential at an atomic site (EPN) is defined as the potential value calculated at that point subtracted by the nuclear term concerning the same site.